Received: 9 March 2022 | Revised: 10 May 2022 | Accepted: 2 June 2022

DOI: 10.1002/nano.202200049

RESEARCH ARTICLE

Nano Select Open Access WILEY

Bacteria (*E. coli*) take up ultrasmall gold nanoparticles (2 nm) as shown by different optical microscopic techniques (CLSM, SIM, STORM)

Nataniel Białas[1] | **Viktoriya Sokolova**[1] | **Selina Beatrice van der Meer**[1] | **Torben Knuschke**[2] | **Tatjana Ruks**[1] | **Kai Klein**[1] | **Astrid M. Westendorf**[2] | **Matthias Epple**[1]

[1]Inorganic Chemistry and Centre for Nanointegration Duisburg-Essen (CENIDE), University of Duisburg-Essen, Essen, Germany

[2]Infection Immunology, Institute of Medical Microbiology, University Hospital Essen, University Duisburg-Essen, Essen, Germany

Correspondence
Matthias Epple, Inorganic Chemistry and Centre for Nanointegration Duisburg-Essen (CENIDE), University of Duisburg-Essen, Essen, Germany.
Email: matthias.epple@uni-due.de

Abstract

The uptake of fluorescently labeled ultrasmall gold nanoparticles (2 nm) by Gram-negative *Escherichia coli* bacteria occurs within 1–3 hours. This was demonstrated by confocal laser scanning microscopy (CLSM), structured illumination microscopy (SIM), stochastic optical reconstruction microscopy (STORM), and flow cytometry. For imaging, eGFP-expressing and DsRed2-expressing *E. coli* strains were used in addition to non-fluorescing *E. coli* strains. Gold nanoparticles were labeled with fluoresceine (FITC), Cy3, and AF647, respectively. Importantly, gold nanoparticles showed no toxicity to the bacteria, indicating a non-lethal nature of the uptake, that is, not related to cell injury.

KEYWORDS
bacteria, gold, microscopy, nanoparticles, uptake

1 | INTRODUCTION

Nanoparticles have a broad range of potential applications in biomedicine, for example in targeted drug delivery, anti-tumor therapy, imaging, and immunization.[1–5] Gold nanoparticles are particularly interesting for a biomedical application, due to their size- and shape-related optical properties like plasmon resonance, autofluorescence,[6–7] photoluminescence,[8] high biocompatibility and low toxicity to cells.[7,9–11] Cellular internalization plays the key role in the interactions between nanoparticles and cells. Therefore, numerous studies have been carried out to better understand the interactions between nanoparticles and cells. The uptake of various types of nanoparticles by eukaryotic cells is now well understood. It is usually based on vesicle-mediated endocytosis or phagocytosis.[12–15] Cluster-sized ultrasmall gold nanoparticles (1–2 nm in core diameter) have a particularly high efficiency for cell penetration, even into the cell nucleus.[16–20]

In contrast to eukaryotic cells, bacteria possess a rigid multilayer cell wall which regulates cell-environment interactions, including particle uptake. Therefore, the uptake of nanoparticles by bacteria is more challenging from both chemical and biological points of view. The antibacterial activity of various nanoparticles, usually of metallic (e.g., silver, copper [4,9,21–24]) or oxidic nature (e.g., zinc oxide[25]) has been thoroughly studied. Typically, the antibacterial effect is ascribed to the release of antibacterial ions like Ag^+ or Zn^{2+} and not to the bacterial uptake of the original nanoparticles.[26–27] In addition, metal ions

TABLE 1 Properties of ultrasmall gold nanoparticles used to study the uptake by bacteria

Sample	Dye molecules per gold nanoparticle	Nanoparticle core diameter by HRTEM/nm	Nanoparticle hydrodynamic diameter by DCS/nm
Au-Cy3 [17,39]	5	1.9 ± 0.2	1.5 ± 0.8
Au-FITC [40]	57	1.7 ± 0.5	1.7 ± 0.5
Au-AF647 [38]	11	2.5 ± 1.1	1.4 ± 0.2

The number of dye molecules per nanoparticle and the nanoparticle concentration are based on an average nanoparticle diameter of 2 nm (gold core) and the assumption of spherical nanoparticles (see Ref.[38] for typical calculations).

may cause damage to the cell membrane, interfere with protein synthesis, inactivate enzymes, and disrupt DNA replication.[28]

In contrast to eukaryotic cells, our knowledge on the uptake of nanoparticles by bacteria is more limited because the mechanism behind cellular internalization of nanoparticles is not well understood. This is mostly due to the fact that bacteria are smaller than eukaryotic cells, so that classical light microscopy (including confocal microscopy) reaches its detection limit when trying to visualize nanoparticles inside bacteria. As alternatives, transmission electron microscopy (TEM)[29–30] and super-resolution microscopy beyond the diffraction limit[31] have been used to address this important question. For example, the detection limit of confocal microscopy is 200 nm at best, whereas it is about 100 and 20 nm for structured illumination microscopy (SIM) and stochastic optical reconstruction microscopy (STORM), respectively.[32–34] Nevertheless, the study of the particle uptake by bacteria is challenging due to a still limited optical resolution and due to artefacts in TEM imaging.[35]

It is expected that the uptake by bacteria occurs more easily for very small nanoparticles. Perspectively, ultrasmall nanoparticles (<2 nm) may act as carriers for the delivery of drugs and antimicrobials into bacteria.[36–37] Here, we show that fluorescently labeled ultrasmall gold nanoparticles (2 nm) can penetrate the cell wall of the Gram-negative bacterium *E. coli* and without cytotoxic side effects. For improved imaging, eGFP-expressing and DsRed2-expressing *E. coli* strains were used.

2 | RESULTS

E. coli bacteria were incubated with ultrasmall gold nanoparticles with different fluorescent labels to assess the interaction. All relevant properties of the applied nanoparticles are summarized in Table 1. The nanoparticle dose was between 10^5 and 10^7 nanoparticles per cell, that is, very high compared to a physiological situation or a nanomedical application. Both nanoparticles and bacteria were dispersed in the medium; therefore, we can expect many contacts between them in the dispersion by collision during diffusion.

Confocal laser scanning microscopy and structured illumination microscopy were applied to study the uptake of nanoparticles by bacteria. Au-FITC nanoparticles were well taken up by *E. coli* (Figure 1). The particles were clustered inside the cells. In contrast, dissolved FITC was not taken up by the bacteria (Figure 2). A detachment of the dye from the nanoparticle surface during the incubation can be excluded due to the strong covalent bond as shown earlier.[17]

The uptake of red-fluorescent Au-Cy3 nanoparticles by green-fluorescent *E. coli* DH5α-eGFP cells gave similar results (Figure 3). The nanoparticles were taken up to a considerable extent by individual bacteria. In contrast to FITC, the dissolved red-fluorescent dye Cy3 was taken up by the bacteria to some extent (Figure 4).

There is the possibility that the penetration of the bacterial membrane by the nanoparticle causes lethal damage to the cells. To assess a potential toxicity of gold nanoparticles towards bacteria, we incubated non-fluorescent *E. coli* DH5α cells with Au-FITC nanoparticles. The green CLSM channel was used for nanoparticle imaging, and the red CLSM channel was used for dead bacteria imaging (propidium iodide; PI). We found that the ultrasmall gold nanoparticles were not toxic to bacteria, as most *E. coli* DH5α cells were still alive (Figure 5).

SIM has a higher resolution than CLSM and is therefore better suited to study bacteria and nanoparticles. SIM images showed a strong red-fluorescence of Au-AF647 nanoparticles inside green-fluorescent *E. coli* DH5α-eGFP cells (Figure 6). The nanoparticles were efficiently taken up by bacteria already after 1 hour incubation. Signals from single nanoparticles localized in the intercellular space were also detected. The particles were well distributed in the cells (cytoplasm). No preferential localization on the cell wall or in the center was observed. Further cultivation of *E. coli* DH5α-eGFP (3 hours) resulted in an increasing number of bacteria. Due to the absence of IPTG, subsequent *E. coli* generations did not produce eGFP, therefore it was not possible to make studies beyond 3 hours.

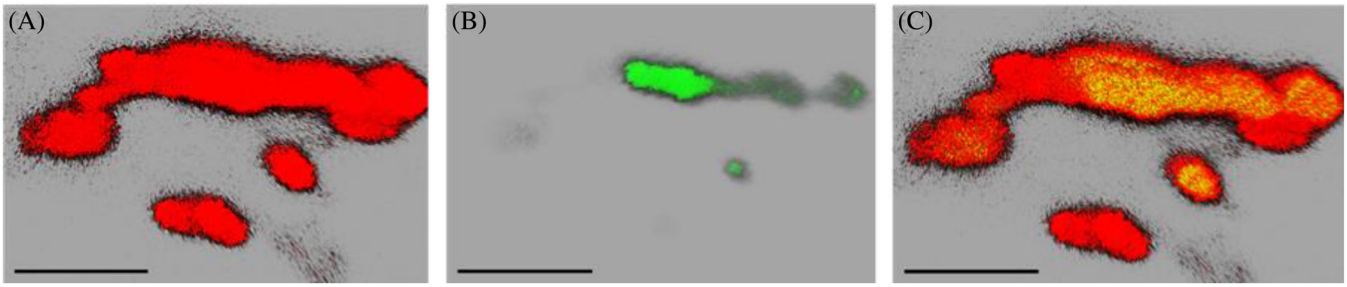

FIGURE 1 Confocal laser scanning microscopy of red-fluorescent *E. coli* TOP10 cells, incubated with green-fluorescent Au-FITC nanoparticles (25 μg mL^{-1}) for 2 hours. A, DsRed2 channel for *E. coli* TOP10; B, FITC channel for nanoparticles; C, Overlay (yellow: Overlay of red and green fluorescence). Scale bars 2 μm

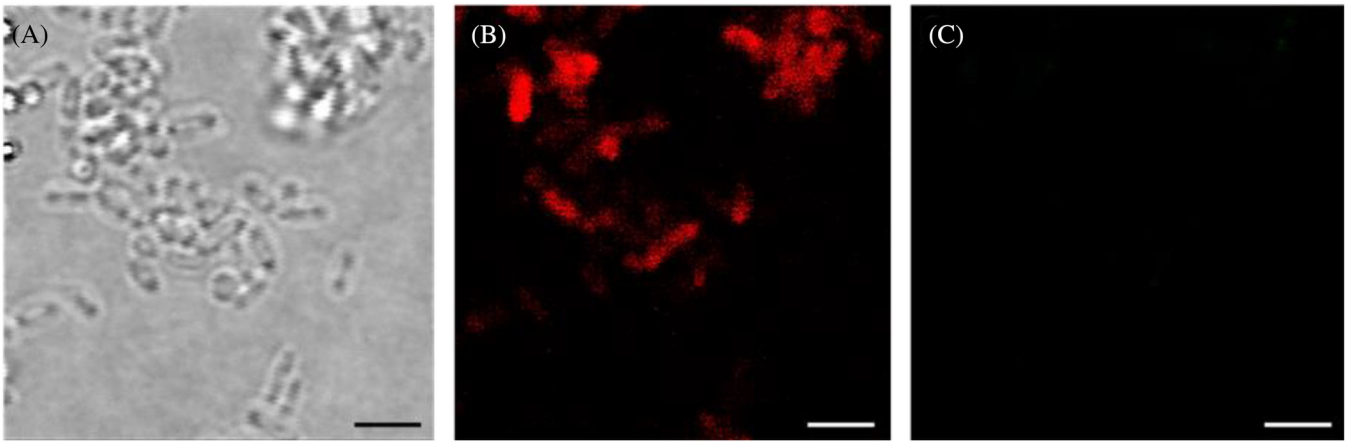

FIGURE 2 Confocal laser scanning microscopy of red-fluorescent *E. coli* TOP10 cells, incubated with dissolved green-fluorescent FITC for 2 hours. The images were taken under the same conditions as with Au-FITC nanoparticles. A, Brightfield channel for *E. coli* TOP 10; B, DsRed2 channel for *E. coli* TOP 10; C, FITC channel. Obviously, all FITC molecules were removed by washing. Scale bars 2 μm

An even higher resolving optical technique is STORM. This method confirmed the suitability of the applied experimental setup (AF488-stained bacteria and AF647-stained nanoparticles) for prolonged imaging (thousands of cycles) based on induced photo-switchability (excited state-dark state) of the applied fluorophores. Figure 7 shows high-resolution images of bacteria and nanoparticles. Binding of the dye AF488 to the bacterial membrane was confirmed, as the green-fluorescent signals corresponded to the localization of the bacterial cell envelope. The red-fluorescing Au-AF647 nanoparticles were detected in the intercellular space (no washing step) and inside the bacteria. However, it must be stressed that STORM does not permit to resolve the data in z-direction as it is possible by CLSM.

Imaging gives only information about few cells. With increasing resolution, the number of analyzed cells decreases. Analysis of bacteria by flow cytometry gives a better statistical image as it permits to analyze thousands of cells of one batch. However, the location of the fluorescing particles (inside a cell or on the surface of a cell) cannot be assessed by this method. Figure 8 shows flow cytometry results on the uptake of red-fluorescent Au-AF647 nanoparticles by green-fluorescent *E. coli* DH5α-eGFP cells after incubation for 1 hour. There is a clear dose-dependent uptake of nanoparticles by bacteria.

3 | DISCUSSION

By a combination of different methods, we have shown that ultrasmall gold nanoparticles are taken up by *E. coli* bacteria within a few hours. To enter the bacteria, nanoparticles or molecules must penetrate the cell wall. Here, fundamental differences exist between Gram-positive and Gram-negative bacteria. The cell wall of Gram-positive bacteria consists of a phospholipid bilayer (cell membrane) tightly covered with a thick multilayer peptidoglycan network, containing covalently bound teichoic, lipoteichoic and teichuronic acids (cell wall thickness up to 80 nm). These are responsible for the negative charge of the cell

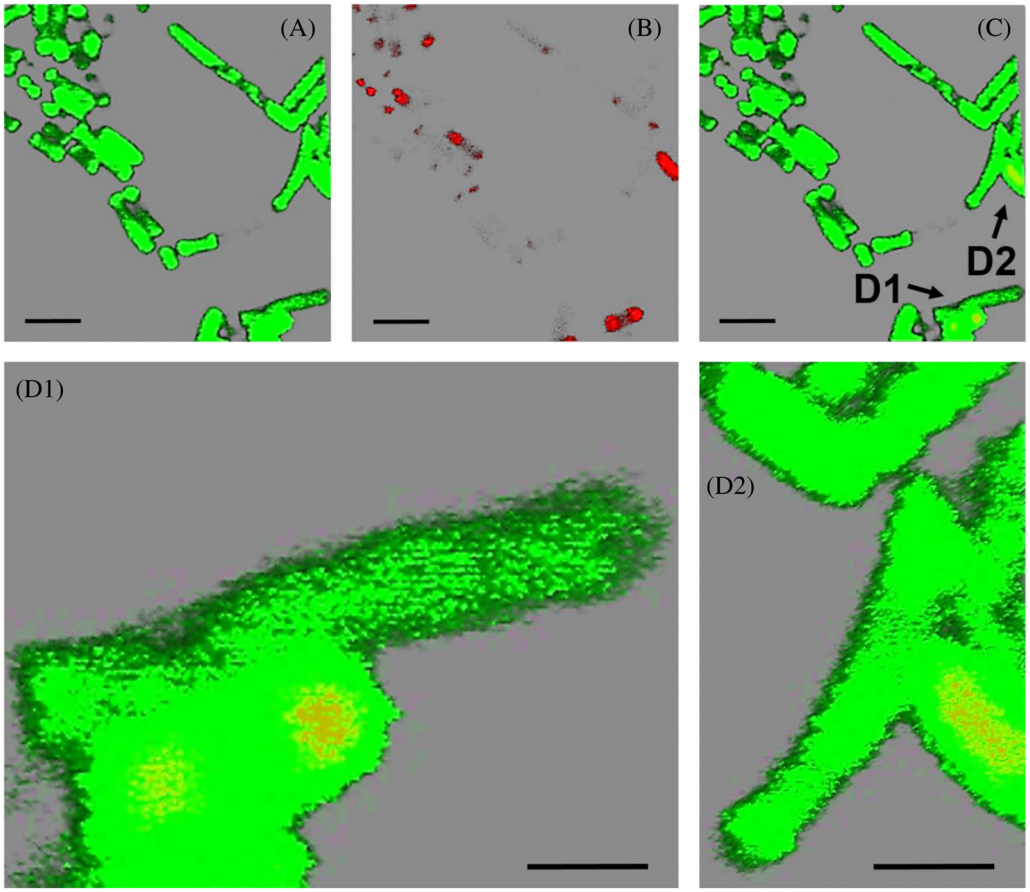

FIGURE 3 Confocal laser scanning microscopy of green-fluorescent *E. coli* DH5α-eGFP cells, incubated with red-fluorescent Au-Cy3 nanoparticles (25 μg mL^{-1}) for 2 hours. Arrows depict cells which took up the nanoparticles. A, GFP channel for *E. coli* DH5α-eGFP; B, Cy3 channel for nanoparticles; C, Overlay; D1-D2, Enlarged images of single bacteria which took up nanoparticles. Scale bars 2 μm (top row) and 1 μm (bottom row)

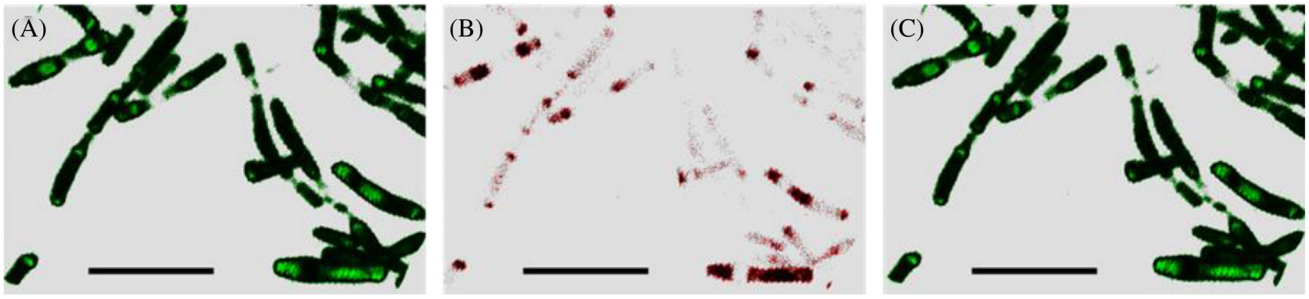

FIGURE 4 Confocal laser scanning microscopy of green-fluorescent *E. coli* DH5α-eGFP, incubated with the dissolved red-fluorescent dye Cy3 for 2 hours. The images were taken at the same conditions as with Au-Cy3 nanoparticles. A, GFP channel for *E. coli* DH5α-eGFP; B, Cy3 channel for Cy3; C, Overlay. Scale bars 2 μm

surface.[41–43] In contrast, the cell wall of Gram-negative bacteria (like *E. coli* studied here) is more complex and consists of two phospholipid bilayers (inner and outer membrane), separated by a peptidoglycan-containing periplasmic space. The peptidoglycan network is limited to just a few layers (thickness of the cell wall up to 10 nm).[44–45]

In Gram-negative bacteria, the presence of two different and metabolically active membranes in the cell wall creates a complex permeability barrier for molecule and particle uptake.[46] Moreover, the surface of Gram-negative bacteria is decorated with glycolipids like lipopolysaccharides (LPS) which provide a strongly negative charge of

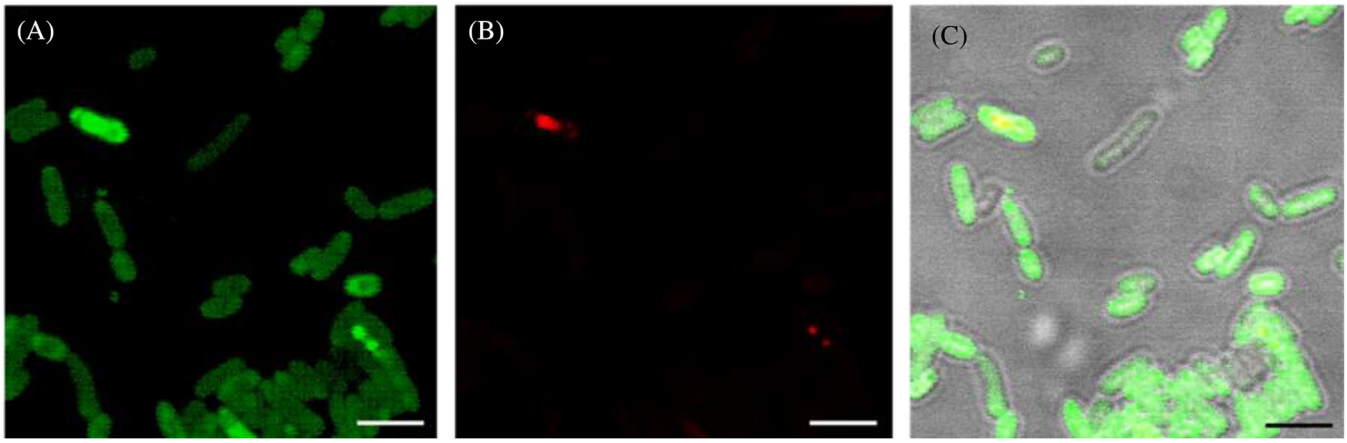

FIGURE 5 Confocal laser scanning microscopy of non-fluorescent *E. coli* DH5α cells, incubated with green-fluorescent Au-FITC nanoparticles (25 μg mL^{-1}) for 2 hours, followed by PI dead staining (red). A, FITC channel for nanoparticles; B, PI channel for dead *E. coli* DH5α cells; C, Overlay (including brightfield). Scale bars 2 μm

the cell surface.[41,47,48] The EPS production by bacteria, either in form of a capsule tightly bound to the cell surface (capsular polysaccharide, CPS) or loosely attached and secreted to the extracellular environment slime, makes particle entrance into bacteria also challenging.[49]

Due to differences in bacterial cell wall structure, the penetration of nanoparticles into Gram-positive and Gram-negative bacteria is expected to be different. As we have studied the Gram-negative species *E. coli*, we will discuss our observations in the context of the literature, also in comparison with Gram-positive species.

The superficial LPS layer of the cell wall outer membrane plays a protective role against antibiotics.[50] It has been suggested that its absence in Gram-positive bacteria could be the reason for the increased cytotoxicity of some nanoparticles compared to Gram-negative bacteria.[51] The complexity of the cell membrane penetration, particularly in Gram-negative bacteria, can be illustrated with antibiotics. Those with cytoplasmic or ribosomal targets in bacteria, first cross the outer membrane by passive diffusion through porin channels and next require an active transport mechanism to further pass the inner membrane and finally reach the bacterial cytoplasm.[52]

Three main mechanisms have been proposed to explain how nanoparticles can cross the bacterial cell envelope: (i) non-specific diffusion (e.g., through β-barrel porin channels in Gram-negative bacteria), (ii) non-specific membrane damage (related to cell injury), and (iii) specific uptake (suitable also for large molecules).[53] Non-specific diffusion is believed to be the leading mechanism for particle uptake in bacteria, however, it is restricted by the cell wall pore diameter and believed to be possible only for particles below 20 nm diameter.[29,53] The average diameter of the cell wall pores in Gram-positive *Bacillus subtilis* and Gram-negative *E. coli* is ~2 and ~4 nm, respectively.[54] Moreover, in *E. coli*, 600 Da is the mass limit for molecules in a pore-mediated uptake.[55] However, the pore size may change during cell division. For instance, in other cell wall-possessing organisms (algae, fungi and plants), the pore size in cell walls increases during cell division and makes the cell wall permeable for larger particles.[56–57]

Some examples of nanoparticle uptake by bacteria have been reported. Kloepfer et al. demonstrated that CdSe quantum dots with a diameter below 5 nm were able to penetrate the cell wall of *B. subtilis* (Gram-positive) and *E. coli* (Gram-negative).[53] Morones et al. concluded that a size range of 1–10 nm is preferential for the uptake of silver nanoparticles by various bacteria (*Salmonella enterica* Typhimurium, *E. coli*, *Vibrio cholerae*, and *P. aeruginosa*; all Gram-negative).[58] Lonhienne et al. have shown that even 10 nm gold nanoparticles were taken up by *Gemmata obscuriglobus* (Gram-negative) However, for *G. obscuriglobus*, a representative of the phylum *Planctomycetes*, a specific uptake mechanism was proposed. Due to the presence of an intracellular membrane system, which is unique among bacteria and *Archaea* and similar to the cell compartment network observed in eukaryotic cells, *G. obscuriglobus* can also internalize larger particles in analogy to endocytosis.[55] Kumar et al. reported the uptake of 5 nm gold nanoparticles by *E. coli* and *S. aureus* (Gram-positive).[59] Interestingly, Feng et al. have shown that gold nanoparticles in the size range of 4–9 nm were not taken up by *B. subtilis* and Gram-negative *Shewanella oneidensis*.[51] Wang et al. demonstrated that 16 nm gold nanoparticles were not taken up by *S. enterica* Typhimurium (Gram-negative).[60] On the other hand, Mohamed et al. showed that even 25 nm gold nanoparticles were able to pass through the cell wall of *Corynebacterium pseudotuberculosis* (Gram-positive).[61] Butler et al. did not observe an uptake of 20 nm titanium dioxide

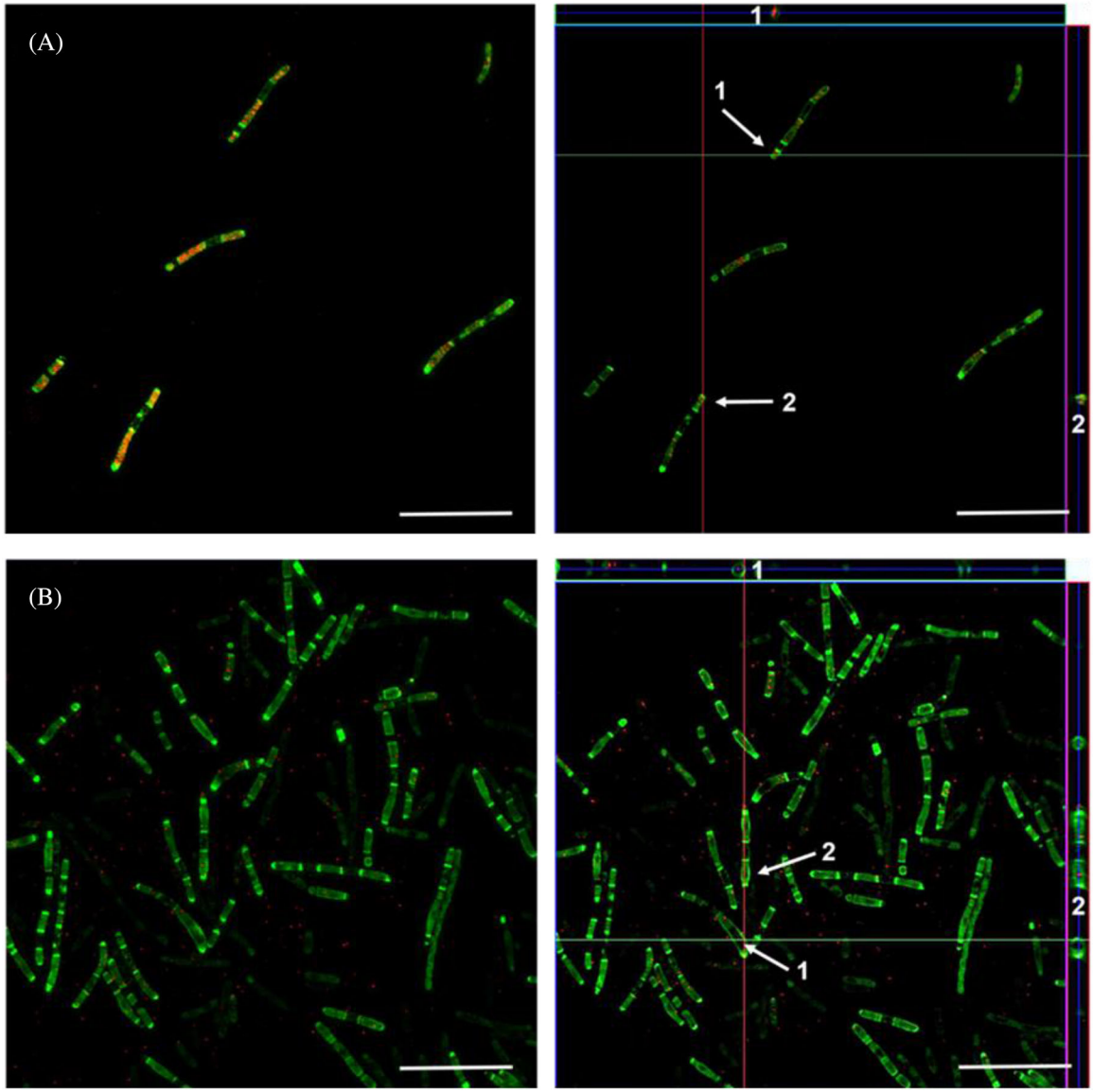

FIGURE 6 SIM images of green-fluorescent *E. coli* DH5α-eGFP cells, incubated with red-fluorescent Au-AF647 nanoparticles (25 μg mL^{-1}) for 1 hour (A) and 3 hours (B). The arrows indicate examples of the intracellular uptake of the nanoparticles by bacteria. SIM-MIP images (left) and SIM-ORTHO projections for intracellular tracking of the nanoparticles (right) are shown. Scale bars correspond to 5 μm

nanoparticles by *S. enterica* Typhimurium (Gram-negative).[62] Pajerski et al. reported that 30 nm gold nanoparticles were not taken up by *Staphylococcus carnosus* (Gram-positive) and *B. subtilis* (Gram-positive), *Neisseria subflava* (Gram-negative), and *Stenotrophomonas maltophilia* (Gram-negative).[63] Sawosz et al. observed that gold nanoparticles (2–30 nm; polydisperse) did not penetrate cells of *Listeria monocytogenes* (Gram-positive) and *Salmonella enterica* Enteritidis (Gram-negative). However, platinum nanoparticles (2–20 nm; polydisperse) entered *L. monocytogenes* (Gram-positive) and *S. enterica* Enteritidis (Gram-negative) after disintegration of the cell wall which confirms a significant cytotoxicity of platinum nanoparticles to bacteria (lethal internalization) in contrast to gold.[64] Zhang et al. reported that gold nanoclusters (Au_{22}) were taken up by non-photosynthetic *Moorella thermoacetica* (Gram-positive).[65]

Although not always consistent, the results indicate that the particle size is a key parameter in nanoparticle internalization by bacteria. The nature of the uptake varies strongly between the bacterial species, but their Gram-affiliation does not appear to play a major role. In our experiments, the small diameter of the ultrasmall gold nanoparticles has helped to penetrate the cell wall of *E. coli*. An important question regarding the size limitation of internalized particles is whether the involved uptake mechanism is passive or active (energy-driven).

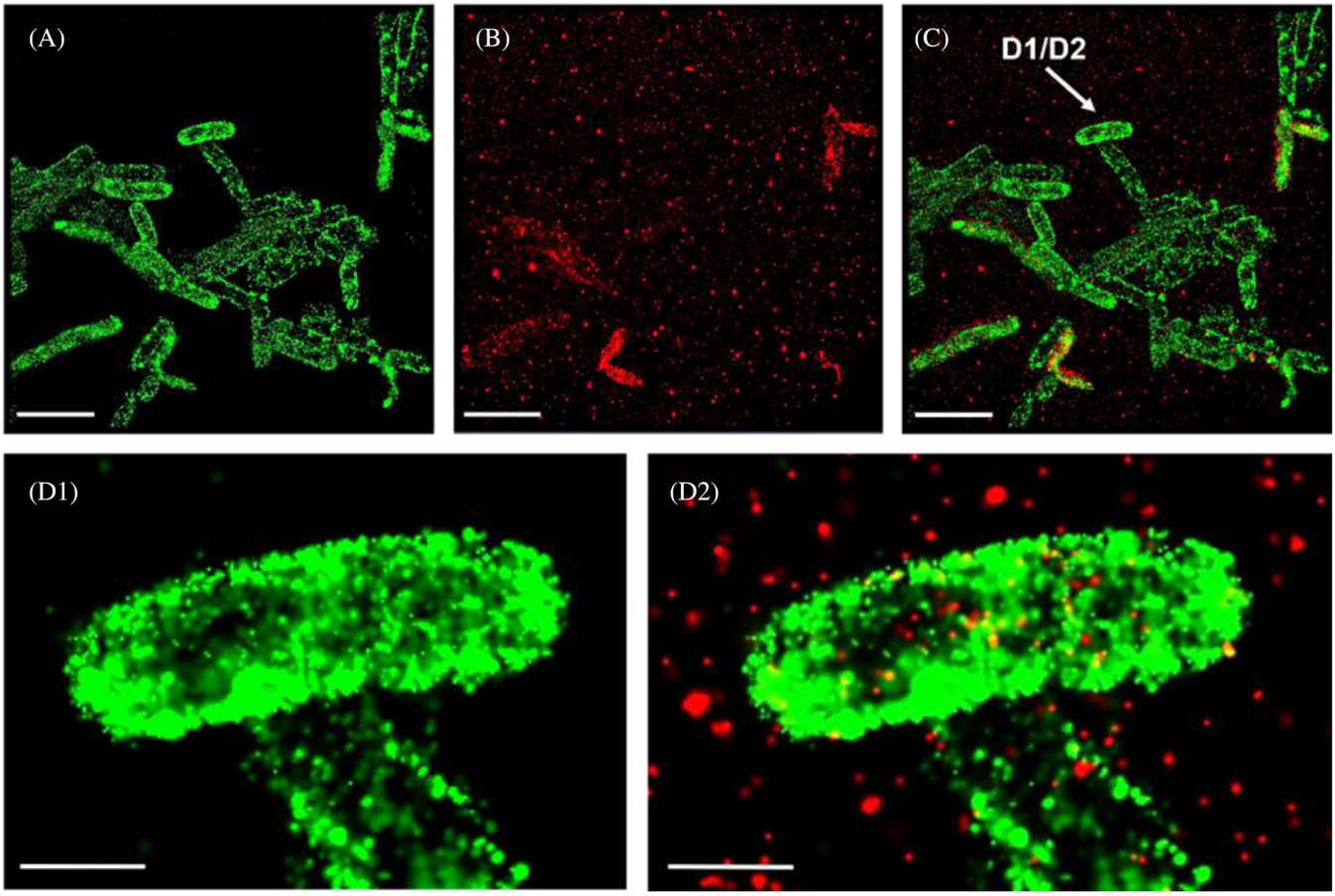

FIGURE 7 STORM images of green-fluorescent *E. coli* DH5α cells (AF488 membrane-stained), incubated with red-fluorescent Au-AF647 nanoparticles (25 μg mL^{-1}) for 2 h. A, AF488 channel for *E. coli* DH5α cells; B, AF647 channel for nanoparticles; C, Overlay; D1-D2, Enlarged images of a single cell (D1; AF488 channel) with incorporated nanoparticles (D2; overlay of AF488 and AF647 channels). Scale bars 1 μm (top row) and 250 nm (bottom row)

The surface nature of the nanoparticles also plays an important role, together with the particle size and charge. Biomolecules (e.g., peptides, proteins or nucleic acids) that are attached to the nanoparticle surface (e.g., a protein corona[66]) play an important role in biorecognition and specific particle uptake, but the effect has been considered minor for ultrasmall particles by Boselli et al.[67]

In terms of the experimental evidence for a nanoparticle uptake, it is often difficult to assess whether particles are inside the cells or on their surface. In this respect, gold nanoparticles are especially well suited for to study uptake mechanisms because they are neither cytotoxic nor membrane-damaging like silver[42,58,68] or platinum.[69–71] The observed absence of cytotoxicity of the ultrasmall gold nanoparticles is in line with the literature. Hayden et al. demonstrated that thiol-stabilized gold nanoparticles (2 nm) rapidly lysed *B. subtilis* cells but not *E. coli*.[72] Boda et al. reported that ultrasmall gold nanoparticles (2 nm) were not cytotoxic to Staphylococci (*S. aureus*, *S. epidermidis*), *E. coli*, and *P. aeruginosa*.[73] Jin et al. suggested that the antibacterial activity of ultrasmall silver nanoparticles could be strain-specific. In the *E. coli* DH5α strain, ultrasmall silver nanoparticles (2 nm) caused outer membrane damage resulting in increased cell wall permeability. The antibacterial activity inside the cell was ascribed to the release of silver ions from the nanoparticles. In the *E. coli* DSM 4230 strain, ultrasmall silver nanoparticles were taken up by cells via porin-mediated diffusion and targeted the respiratory chain at the inner membrane level. However, an antibacterial effect of these nanoparticles on *S. aureus* was not observed.[68] This mechanism was also suggested by Morones et al. for *E. coli* (strain not reported), *S. enterica* Typhimurium, *V. cholerae*, and *P. aeruginosa*, incubated with silver nanoparticles.[58]

We have shown here that only a combination of several methods permits to draw conclusions on the actual degree of bacterial uptake. Ultrasmall nanoparticles can penetrate the bacterial cell wall more easily, but even optical super-microscopy reaches its limits. Transmission electron microscopy of ultrasmall nanoparticles requires high-resolution aberration-corrected instruments[38] which cannot be applied to metal-stained bacteria without

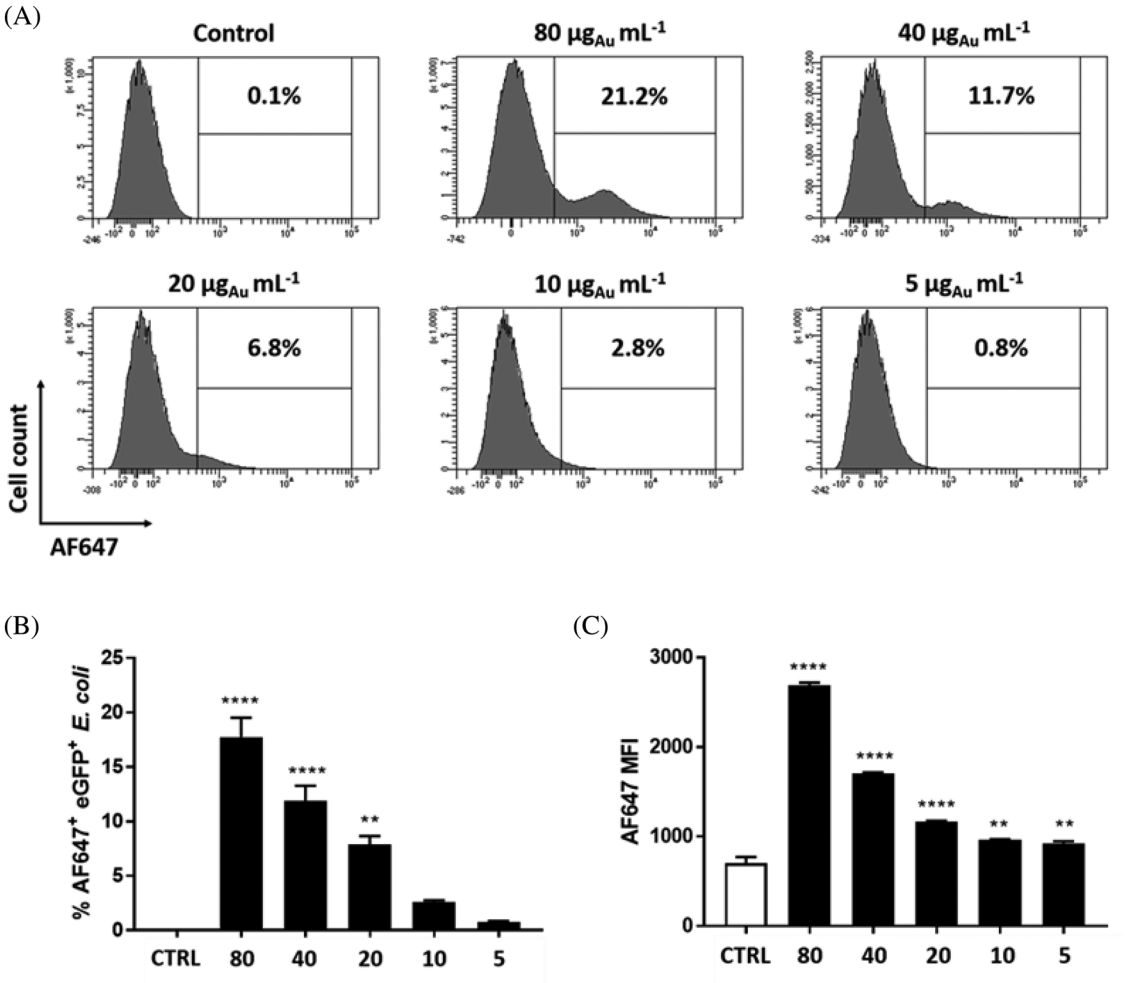

FIGURE 8 Flow cytometry of green-fluorescent *E. coli* DH5α-eGFP cells, incubated with red-fluorescent Au-AF647 nanoparticles for 1 hour. Representative flow cytometry results (A), percentage of nanoparticle-positive bacteria (B), and mean fluorescence intensity (MFI) values of AF647 (from internalized nanoparticles) (C) are shown. In B and C, nanoparticle concentrations are given in μg mL^{-1}. Data shown are mean ± SEM. *p* values indicate significant differences to control bacteria (not exposed to the nanoparticles) with $p < 0.01$ (**) or $p < 0.0001$ (****) ($N = 3$)

the occurrence of artefacts, for example by osmium, uranium, or lead staining.[74]

For a biomedical application, it is interesting that nanoparticles tend to increase the permeability of bacterial cell wall membranes which may result in an enhanced uptake of antibiotics.[37,75] This is an emerging topic because due to the rapid development and spread of drug resistance among bacteria, there is a lack of new and effective antibiotics,[76] and a need to develop novel platforms for antimicrobial drug delivery.[75,77] It has been reported that gentamicin[78] and azithromycin[79] were more effective against enteropathogenic *S. enterica* Typhimurium when delivered to cells by polymeric nanoparticles compared to the dissolved antibiotics. A similar effect was observed in *S. aureus*, a skin-associated opportunistic pathogen, for nanoparticles loaded with clarithromycin.[80] Ultrasmall gold nanoparticles do not appear to damage the bacterial cell wall, but they may be well suited as carriers for drugs or antimicrobials into a bacterium.

4 | CONCLUSIONS

We have shown by a combination of methods, that is confocal laser scanning microscopy (CLSM), structured illumination microscopy (SIM), stochastic optical reconstruction microscopy (STORM), and flow cytometry, that Gram-negative *E. coli* bacteria take up ultrasmall gold nanoparticles (2 nm; labeled with the fluorescent dyes Cy3, FITC, and AlexaFluor-647). This is the first report on the application of super-resolution microscopy to bacteria-nanoparticle investigations. Fluorescently labeled ultrasmall gold nanoparticles were taken up by fluorescent

E. coli strains DH5α, DH5α-eGFP and TOP10. The uptake efficiency increased with increasing particle dose. However, it must be noted that the nanoparticle concentration that was applied here was rather high and will probably be lower for any therapeutic application. Due to the very small size of the nanoparticles, we assume that they were internalized via non-specific pore-mediated diffusion. Ultrasmall gold nanoparticles were not toxic to the bacteria, that is a penetration by membrane damage as reported for silver and platinum is unlikely. Thus, fluorescently labeled ultrasmall gold nanoparticles are promising tools to study the uptake of particles from the environment by bacteria (without causing lethal effects), possibly for a future nanomedical application.

5 | METHODS

5.1 | Gold nanoparticles

Ultrapure water (Purelab ultra instrument from ELGA) was used for all syntheses, analyzes and procedures unless otherwise noted.

Ultrasmall gold nanoparticles were covalently functionalized[17] with the dye Cy3 (Au-Click-Cy3) by click chemistry (copper-catalysed azide-alkyne cycloaddition; CuAAC), following earlier reported syntheses.[81–82] AlexaFluor-647 (abbreviated as AF647 in the following) was attached by clicking on azide-terminated gold nanoparticles (2 nm)[38] to yield Au-AF647 nanoparticles. The synthesis of ultrasmall gold nanoparticles labeled with FITC (Au-FITC) was a two-step process. First, ultrasmall gold nanoparticles were functionalized with glutathione (Au-GSH). In the second step NHS-fluorescein was coupled to the primary amine group of Au-GSH.[40]

For both kinds of nanoparticles, the gold content of the nanoparticle dispersions was determined by atomic absorption spectroscopy (AAS) and converted to the number of gold nanoparticles, using the density of gold and the average particle diameter (solid core) of 2 nm. As each gold nanoparticle has a weight of 8.08×10^{-20} g (about 250 Au atoms per particle), 1 g of gold nanoparticles corresponds to 1.24×10^{19} particles. The amount of dye was measured by UV-vis and fluorescence spectroscopy, using calibration curves from dye solutions (see Ref.[17] for a typical calculation).

5.2 | Bacterial strains

All experiments were performed with sterile materials and labware. Ultrapure water (Purelab ultra instrument from ELGA) was used for all synthetic procedures involving nanoparticles.

We used the Gram-negative *E. coli* DH5α strain (non-fluorescent, parental strain) and two fluorescent *E. coli* strains, that is DH5α-eGFP (eGFP-expressing bacteria; green fluorescence) and TOP10 (DsRed2-expressing bacteria; red fluorescence; obtained from Prof. Wiebke Hansen, University Hospital Essen). The *E. coli* DH5α strain was cultivated in lysogeny broth (LB), whereas the strains DH5α-eGFP and TOP10 required an LB medium supplemented with ampicillin (100 mg L^{-1}). LB medium was prepared by addition of agar-agar Kobe I (15 g L^{-1}). All growth media and chemicals were purchased from Carl Roth (Germany). All bacterial strains were grown at 37°C with orbital shaking at 130 rpm (ThermoScientific, MAXQ 4000).

For the preparation of electrocompetent *E. coli* DH5α cells and all further experiments with the strains *E. coli* DH5α and *E. coli* DH5α-eGFP, log-phase bacterial cultures were prepared from overnight cultures. 49 mL medium were inoculated with 1 mL of an overnight culture (2% inoculum) and grown until the fresh culture reached the optical density (OD) of 0.6 (measured by turbidimetry at 600 nm; WPA Biowave, CO8000 Cell Density Meter; McFarland turbidity standards were used as reference). Bacteria were made electrocompetent as follows. 50 mL of a log-phase *E. coli* DH5α culture were incubated on ice for 15 minutes and isolated by centrifugation (ThermoScientific, Multifuge X1R; 4000 rpm, 10 minutes, 4°C). The pellet of bacteria was resuspended in 50 mL, followed by the addition of 25 mL cold water, thorough vortexing (Scientific Industries, Vortex-Genie 2), and again centrifugation. The pellet was resuspended in 5 mL of cold 10/90 glycerol/water (Carl Roth), vortexed and centrifuged. Finally, the pellet was resuspended in 2.5 mL of cold 10/90 glycerol/water, vortexed and aliquoted. The electrocompetent *E. coli* DH5α cells were immediately frozen and stored at -80°C.

For the transformation of bacteria, 39 µL of electrocompetent *E. coli* DH5α cell dispersion were thoroughly mixed with 1 µL (115 ng) of eGFP- and ampicillin-resistance-carrying plasmid DNA (pGEX-6P-1, 5.7 kb, containing the lac operon) and incubated for 1 minute on ice. The sample was transferred to a pre-cooled electroporation cuvette (Biorad, GenePulser Cuvette; 0.2 cm, gap 5) and transformed with an electric pulse (Biorad, Gene Pulser Xcell; 25 µF, 1.8 kV, 5 ms). After electroporation, 900 µL of LB medium pre-warmed to 37°C was immediately added to the transformed bacteria, then the sample was transferred to a new tube and incubated with intensive shaking at 37°C for 1 hour. The culture was centrifuged (Eppendorf Centrifuge 5430; 4000 rpm, 10 minutes, room temperature), 2/3 of the supernatant was removed, and

the remaining volume of the supernatant was used to resuspend the bacterial pellet. 150 µL of the bacterial suspension was plated on ampicillin-containing LB agar plate and incubated overnight at 37°C for the isolation of eGFP plasmid-positive bacterial colonies. A pure liquid culture of transformed *E. coli* DH5α-eGFP cells was prepared from a single colony after performing streak plating, mixed thoroughly with glycerol as cryoprotective agent (1:4 = *v*/*v*), aliquoted, immediately frozen, and stored at -80°C.

For the stimulation of eGFP expression in bacteria, isopropyl-β-D-thiogalactopyranoside (IPTG; Carl Roth) was used. On the molecular level, IPTG mimics allolactose which is the natural activator of lac operon transcription. The activation results in the expression of proteins encoded by genes being controlled by the lac operon.[83] IPTG was added to 50 mL of a log-phase *E. coli* DH5α-eGFP culture (prepared as described above) to a concentration of 0.4 mM. Bacteria were grown overnight at 30°C with orbital shaking at 130 rpm. Fluorescence microscopy (Keyence, Biorevo BZ-9000) confirmed the efficient eGFP expression by IPTG-stimulated bacteria.

In *E. coli* TOP10 cells, the expression of the fluorescent protein DsRed2 occurs constantly in cells during the bacterial growth. An intense expression of DsRed2 in *E. coli* TOP10 cells was observed after 48 hours of bacterial growth. For all experiments with the strain *E. coli* TOP10, 48 hours cultures were diluted with fresh growth media to obtain bacterial cultures with an OD of 0.6.

5.3 | Incubation of bacteria with nanoparticles and analysis by confocal laser scanning microscopy (CLSM)

0.2 mL (1×10^9 CFU mL^{-1}) of bacterial cultures of the *E. coli* strains DH5α, DH5α-eGFP, and TOP10, respectively, were mixed with dispersions of Au-Cy3 (10 µL; 0.5 mg Au mL^{-1}) or Au-FITC (20 µL; 0.25 mg Au mL^{-1}), respectively. This gave a final dose of nanoparticles for the incubation of 5 µg per well and about 25 µg mL^{-1}.

With an average nanoparticle diameter of 2 nm, this corresponds to 3.1×10^{14} nanoparticles per mL in the well. With 1×10^9 bacteria per mL, the dose was about 3.1×10^5 nanoparticles per cell. Note that this number is an approximation as the number of bacteria increased continuously during the experiment due to cell division (the generation time of *E. coli* under optimal laboratory conditions is ~20 minutes).[84]

The bacteria were incubated with nanoparticles for 2 hours at 37°C with orbital shaking (130 rpm) in darkness, and then prepared for confocal laser scanning microscopy. 20 µL of the sample (bacteria + nanoparticles) was placed on a square glass coverslip (Carl Roth; 18×18 mm^2, thickness 170 ± 5 µm) and left to dry at room temperature in darkness. Next, the bacteria were fixed with 4% formaldehyde (Merck, pH 7.4) for 8 minutes at 37°C, the sample was carefully rinsed twice with water and again left to dry at room temperature in darkness. Next, 20 µL of the mounting medium (Invitrogen, Fluoromount-G) was placed on a glass microscopy slide (ThermoScientific, 76×26 mm^2) and the coverslip was put on the microscopy slide in a way that the surface with the dried sample was carefully immersed, avoiding air bubbles, in the mounting medium. After this procedure, the samples were studied by confocal laser scanning microscopy (Leica TCS SP8 HCS A) and stored, protected from drying, at 4°C in darkness. Glass coverslips and microscopy slides were cleaned with 99% ethanol and water before preparation of the CLSM samples. The laser lines used for excitation were Argon 488 nm (FITC, detection range 488–520 nm) and DPSS 514 nm (Cy3 and propidium iodide; detection range 535–561 nm). Images were acquired with an HCX PL Apo 63x/1.4 oil objective. To study the uptake of the nanoparticles within the cells, z-stacks were acquired (step size 0.1 µm).

For comparison, bacteria were also incubated with the dissolved fluorescent dyes FITC and Cy3. All experimental conditions were the same as in the nanoparticle incubation studies. Instead of nanoparticle dispersions, aqueous dye solutions of the same volume were used. The bacteria were mixed with 10 µL of 50 µM Cy3 solution (final dye concentration in the well: 2.5 µM) or 20 µL of 85 µM FITC solution (final dye concentration in the well: 8.5 µM). Imaging of the samples was performed by CLSM as described above.

To evaluate the cytotoxicity of gold nanoparticles, non-fluorescent *E. coli* DH5α cells were incubated with Au-FITC nanoparticles under the same conditions as above. After incubation and prior to preparation of samples for CLSM imaging (as described above), bacterial cultures were stained with propidium iodide (PI), according to the manufacturer's protocol, for detection of the dead cells. PI is a membrane-impermeable dye, which binds to double-stranded DNA by intercalation.[85] It is used as dead cell marker in commercially available Live/Dead staining kits for evaluation of cell viability. We used the Live/Dead® *Bac*Light Bacterial Viability Kit L7012 (Invitrogen). A crosstalk between the green and red CLSM channel was not observed. Furthermore, untreated *E. coli* DH5α cells were not visible in the fluorescent channels.

5.4 | Incubation of bacteria with nanoparticles and analysis by structured illumination microscopy (SIM)

A total of 0.2 mL (1.5×10^8 CFU mL^{-1}) of bacterial cultures of *E. coli* DH5α-eGFP were mixed with a dispersion

of Au-AF647 nanoparticles (5 µL; 1 mg Au mL^{-1}). This gave a dose of 5 µg gold per well and a concentration of about 25 µg gold per mL, corresponding to 3.1×10^{14} nanoparticles per mL. With 1.5×10^8 bacteria per mL, the dose was about 2.1×10^6 nanoparticles per cell. Note that this number is an approximation as the number of bacteria increased during the experiment. The bacteria were incubated with nanoparticles for 1 or 3 hours at 37°C under orbital shaking (130 rpm) in darkness, and then prepared for SIM. 20 µL of the sample (bacteria + nanoparticles) was placed on a square glass coverslip (Carl Roth; 18×18 mm^2, thickness 170 ± 5 µm) and left to dry at room temperature in darkness. Next, the bacteria were fixed with 4% formaldehyde (Merck, pH 7.4) for 8 minutes at 37°C, the sample was carefully rinsed twice with water and left to dry at room temperature in darkness. Next, 20 µL of the mounting medium (Invitrogen, Fluoromount-G) was placed on a glass microscopy slide (ThermoScientific, 76×26 mm^2) and the coverslip was put on the microscopy slide in a way that the surface with the dried sample was carefully immersed, avoiding air bubbles, in the mounting medium. After this procedure, the samples were studied by SIM (Zeiss Elyra PS.1 instrument) and stored, protected from drying, at 4°C in darkness. Glass coverslips and microscopy slides were cleaned with 99% ethanol and water before preparation of the SIM samples.

The laser lines used for excitation were OPSL 488 nm (eGFP, detection range 495–575 nm; 200 mV) and Diode 642 nm (AF647; detection at 655 nm; 150 mV). Images were acquired with an alpha Plan-Apochromat 100x/1.46 Oil DIC M27 Elyra objective. Z-stacks were acquired (step size 0.1 µm). SIM processing of images was performed with the ZEN system 2012 software. No crosstalk between the eGFP and AF647 channels was observed. Bacteria were not visible in the channel for nanoparticles and vice versa.

SIM images are presented as maximum intensity projections (MIP). With the ORTHO projection of SIM z-stacks, we were able to confirm the intracellular localization of the nanoparticles.

5.5 | Incubation of bacteria with nanoparticles and analysis by stochastic optical reconstruction microscopy (STORM)

For STORM imaging, the autofluorescent eGFP-producing *E. coli* strain could not be used because this super-resolution microscopy technique requires the application of more photostable fluorophores.[86] The photostability of eGFP is not sufficient for STORM imaging. Therefore, the membrane of non-fluorescent *E. coli* DH5α cells (1.5×10^8 CFU mL^{-1}) was chemically labeled with Alexa Fluor-NHS-ester (AF488; Lumiprobe, Germany) according to the protocol described by Turner et al.[87] Bacteria were labeled before incubation with the nanoparticles. NHS-esters are amino group-specific and bind covalently to free amine functional groups of protein amino acids, particularly lysines, in the bacterial cell membranes.[88] Next, *E. coli* DH5α cells (stained with AF488) were incubated with Au-AF647 nanoparticles for 2 hours. The dose of nanoparticles added to the bacterial suspensions and the incubation conditions were the same as in the CLSM and SIM experiments described above. To remove excess nanoparticles after incubation of the bacteria, the bacterial suspension was washed twice with water and centrifuged (4000 rpm, 10 minutes, RT).

For imaging, 30 µL of the sample (bacteria + nanoparticles) were placed on a round glass coverslip with round fiducials (diameter 25 mm, thickness 170 ± 5 µm) and left to dry at room temperature in darkness. Next, the bacteria were fixed with 4% formaldehyde (Merck, pH 7.4) for 8 minutes at 37°C, the sample was carefully rinsed twice with water and then left to dry at room temperature in darkness. As STORM measurements require a constant immersion of the sample in the oxygen-scavenging buffer, and the bacteria are not adherent, particular attention was paid during the sample preparation to a delicate handling of the samples with liquids and a thorough drying of the samples after each rinsing step.

The samples were studied by STORM (Zeiss Elyra PS.1 instrument) in a closed chamber system. The freshly prepared oxygen-scavenging buffer was added to the sample in the chamber directly before imaging.[89] Up to 30,000 frames were recorded with a built-in EMCCD camera with exposure times of up to 100 ms. After imaging, the samples were stored in the dried state at 4°C in darkness. The laser lines used for excitation of the fluorophores were the same as those used for SIM imaging (see above). Excitation of AF488 was performed under the same conditions as the excitation of eGFP. Images were acquired with an alpha Plan-Apochromat 100x/1.46 Oil DIC M27 Elyra objective. STORM processing of the images was performed with the ZEN system 2012 software. STORM images are presented as MIP projections.

5.6 | Incubation of bacteria with nanoparticles and analysis by flow cytometry

A total of 1 mL (1.5×10^8 CFU mL^{-1}) of *E. coli* DH5α-eGFP cultures was mixed with dispersions of Au-AF647 nanoparticles (5, 10, 20, 40, and 80 µL; 1 mg Au mL^{-1}). By assuming an average nanoparticle diameter of 2 nm, this corresponds to a nanoparticle dose of 6.2×10^{13}–9.9×10^{14} particles

per mL, or about 4.1×10^5–6.6×10^6 particles per cell. Note that this number is an approximation as the number of bacteria increases during the experiment. The bacteria were incubated with nanoparticles for 1 hour at 37°C in darkness. Next, the bacteria were fixed with 4% formaldehyde (Merck, pH 7.4) for 8 minutes at 37°C and washed twice with ultrapure water. During fixation and washing steps, bacteria were harvested by centrifugation (ThermoScientific, Heraeus Fresco 21; 5000 rpm, 10 minutes, room temperature). Finally, bacteria were resuspended in 0.3 mL PBS with 2% fetal calf serum (FCS, Sigma Aldrich) and 2 mM ethylenediaminetetraacetic acid (EDTA, Carl Roth) (4°C). All samples were prepared in triplicates. As negative control, untreated *E. coli* DH5α-eGFP cells were used. The uptake of the nanoparticles by bacteria was quantified with an LSR II instrument (BD Biosciences). The frequencies of AF647-positive eGFP-expressing bacteria as well as the mean fluorescence intensity (MFI) were analyzed with the DIVA software (BD Biosciences). Statistical analysis was performed by ordinary one-way ANOVA followed by Tukey's multiple comparisons test.

ACKNOWLEDGMENTS

We thank Prof. Dr. Wiebke Hansen (University Hospital Essen) and Dr. Sebastian Kollenda (University of Duisburg-Essen) for providing the DsRed2-expressing strain *E. coli* TOP10 and the eGFP-plasmid DNA for transformation of bacteria, respectively. We thank Ms. Alexandra Brenzel and Dr. Anthony Squire (Imaging Center Essen, University Hospital Essen) for technical assistance by SIM imaging. M.E. and A.M.W. thank the Deutsche Forschungsgemeinschaft (DFG) for funding within the projects Ep 22/56-1 and We 4472/8-1. We thank the Imaging Center Campus Essen (ICCE) for access to the confocal laser scanning microscopes (CLSM) and the Imaging Center Essen (IMCES) for access to structured illumination microscopy (SIM) and stochastic optical reconstruction microscopy (STORM).

Open access funding enabled and organized by Projekt DEAL.

REFERENCES

1. N. Bertrand, J. Wu, X. Xu, N. Kamaly, O. C. Farokhzad, *Adv. Drug Deliv. Rev.* **2014**, *66*, 2.
2. K. Jeevanandam, A. Barhoum, Y. S. Chan, A. Dufresne, M. K. Danquah, *Beilstein J. Nanotechnol.* **2018**, *9*, 1050.
3. M. G. Manera, A. Colombelli, A. Taurino, A. G. Martin, R. Rella, *Sci. Rep.* **2018**, *8*, 12640.
4. B. Pelaz, C. Alexiou, R. A. Alvarez-Puebla, F. Alves, A. M. Andrews, S. Ashraf, L. P. Balogh, L. Ballerini, A. Bestetti, C. Brendel, S. Bosi, M. Carril, W. C. W. Chan, C. Chen, X. Chen, X. Chen, Z. Cheng, D. Cui, J. Du, C. Dullin, A. Escudero, N. Feliu, M. Gao, M. George, Y. Gogotsi, A. Grünweller, Z. Gu, N. J. Halas, N. Hampp, R. K. Hartmann, et al., *ACS nano* **2017**, *11*, 2313.
5. S. Shamaila, N. Zafar, S. Riaz, R. Sharif, J. Nazir, S. Naseem, *Nanomaterials* **2016**, *6*, 71.
6. C. J. Zeng, *Pure Appl. Chem.* **2018**, *90*, 1409.
7. K. A. Willets, A. J. Wilson, V. Sundaresan, P. B. Joshi, *Chem. Rev.* **2017**, *117*, 7538.
8. M. Tang, J. Zhang, C. Yang, Y. Zheng, H. Jiang, *Front. Chem.* **2020**, *8*, 181.
9. K. M. Rice, G. K. Ginjupalli, N. Manne, C. B. Jones, E. R. Blough, *Nanotechnology* **2019**, *30*, 372001.
10. G. Schmid, W. G. Kreyling, U. Simon, *Arch. Toxicol.* **2017**, *91*, 3011.
11. L. M. M. Neto, A. Kipnis, A. P. Junqueira-Kipnis, *Front. Immunol.* **2017**, *8*, 239.
12. S. Patel, J. Kim, M. Herrera, A. Mukherjee, A. V. Kabanov, G. Sahay, *Adv. Drug Deliv. Rev.* **2019**, *144*, 90.
13. C. M. Beddoes, C. P. Case, W. H. Briscoe, *Adv. Coll. Interface Sci.* **2015**, *218*, 48.
14. N. Feliu, X. Sun, R. A. Alvarez Puebla, W. J. Parak, *Langmuir* **2017**, *33*, 6639.
15. H. H. Gustafson, D. Holt-Casper, D. W. Grainger, H. Ghandehari, *Nano Today* **2015**, *10*, 487.
16. K. Zarschler, L. Rocks, N. Licciardello, L. Boselli, E. Polo, K. P. Garcia, L. De Cola, H. Stephan, K. A. Dawson, *Nanomedicine* **2016**, *12*, 1663.
17. S. B. van der Meer, K. Loza, K. Wey, M. Heggen, C. Beuck, P. Bayer, M. Epple, *Langmuir* **2019**, *35*, 7191.
18. S. Huo, S. Jin, X. Ma, X. Xue, K. Yang, A. Kumar, P. C. Wang, J. Zhang, Z. Hu, X. J. Liang, *ACS Nano* **2014**, *8*, 5852.
19. L. Yang, L. Shang, G. U. Nienhaus, *Nanoscale* **2013**, *5*, 1537.
20. K. Huang, H. Ma, J. Liu, S. Huo, A. Kumar, T. Wei, X. Zhang, S. Jin, Y. Gan, P. C. Wang, S. He, X. Zhang, X. J. Liang, *ACS Nano* **2012**, *6*, 4483.
21. G. Franci, A. Falanga, S. Galdiero, L. Palomba, M. Rai, G. Morelli, M. Galdiero, *Molecules* **2015**, *20*, 8856.
22. K. Bazaka, M. V. Jacob, W. Chrzanowski, K. Ostrikov, *RSC Adv.* **2015**, *5*, 48739.
23. S. Chernousova, M. Epple, *Angew. Chem. Int. Ed.* **2013**, *52*, 1636.
24. S. Galdiero, A. Falanga, M. Vitiello, M. Cantisani, V. Marra, M. Galdiero, *Molecules* **2011**, *16*, 8894.
25. A. Sirelkhatim, S. Mahmud, A. Seeni, N. H. M. Kaus, L. C. Ann, S. K. M. Bakhori, H. Hasan, D. Mohamad, *Nano-Micro Lett.* **2015**, *7*, 219.
26. Z. M. Xiu, Q. B. Zhang, H. L. Puppala, V. L. Colvin, P. J. J. Alvarez, *Nano Lett.* **2012**, *12*, 4271.
27. K. Loza, C. Sengstock, S. Chernousova, M. Koeller, M. Epple, *RSC Adv.* **2014**, *4*, 35290.
28. K. P. Miller, L. Wang, B. C. Benicewicz, A. W. Decho, *Chem. Soc. Rev.* **2015**, *44*, 7787.
29. K. S. Butler, D. J. Peeler, B. J. Casey, B. J. Dair, R. K. Elespuru, *Mutagenesis* **2015**, *30*, 577.
30. L. Mei, Z. Lu, W. Zhang, Z. Wu, X. Zhang, Y. Wang, Y. Luo, C. Li, Y. Jia, *Biomaterials* **2013**, *34*, 10328.
31. C. Coltharp, J. Xiao, *Cell Microbiol.* **2012**, *14*, 1808.
32. N. Feiner-Gracia, S. Pujals, P. Delcanale, L. Albertazzi, in *Smart Nanoparticles for Biomedicine*, G. Ciofani (Ed.), Elsevier **2018**, pp. 219–236.
33. L. A. Trinh, S. E. Fraser, in *Current Topics in Developmental Biology*, Y. Chai (Ed.) Academic Press **2015**, pp. 599–629.
34. R. Henriques, M. M. Mhlanga, *Biotechnol. J.* **2009**, *4*, 846.

35. A. Alabresm, A. W. Decho, J. Lead, *Nanoimpact* **2021**, *21*, 11.
36. A. Gupta, S. Mumtaz, C. H. Li, I. Hussain, V. M. Rotello, *Chem. Soc. Rev.* **2019**, *48*, 415.
37. P. Jelinkova, A. Mazumdar, V. P. Sur, S. Kociova, K. Dolezelikova, A. M. J. Jimenez, Z. Koudelkova, P. K. Mishra, K. Smerkova, Z. Heger, M. Vaculovicova, A. Moulick, V. Adam, *J. Control. Release* **2019**, *307*, 166.
38. K. Klein, K. Loza, M. Heggen, M. Epple, *Chem. Nano. Mat.* **2021**, *7*, 1330.
39. V. Sokolova, G. Nzou, S. B. van der Meer, T. Ruks, M. Heggen, K. Loza, N. Hagemann, F. Murke, B. Giebel, D. M. Hermann, A. J. Atala, M. Epple, *Acta Biomater.* **2020**, *111*, 349.
40. S. Hosseini, O. Wetzel, K. Kostka, M. Heggen, K. Loza, M. Epple, *Molecules* **2021**, *26*, 5069.
41. Y. N. Slavin, J. Asnis, U. O. Häfeli, H. Bach, *J. Nanobiotechnol.* **2017**, *15*, 65.
42. C. Liao, Y. Li, S. C. Tjong, *Int. J. Mol. Sci.* **2019**, *20*, 449.
43. N. Nino-Martinez, M. F. Salas Orozco, G. A. Martínez-Castanon, F. Torres Mendez, F. Ruiz, *Int. J. Mol. Sci.* **2019**, *20*, 2808.
44. A. Mai-Prochnow, M. Clauson, J. Hong, A. B. Murphy, *Sci. Rep.* **2016**, *6*, 38610.
45. B. J. Swift, F. Baneyx, *PLoS One* **2015**, *10*, e0124916.
46. J. Vergalli, I. V. Bodrenko, M. Masi, L. Moynie, S. Acosta-Gutierrez, J. H. Naismith, A. Davin-Regli, M. Ceccarelli, van den B. Berg, M. Winterhalter, J. M. Pages, *Nat. Rev. Microbiol.* **2020**, *18*, 164.
47. A. M. Mitchell, T. Srikumar, T. J. Silhavy, *mBio.* **2018**, *9*, e01321.
48. N. Bialas, K. Kasperkiewicz, J. Radziejewska-Lebrecht, M. Skurnik, *Arch. Immunol. Ther. Exp.* **2012**, *60*, 199.
49. Z. Yang, S. Li, X. Zhang, X. Zeng, D. Li, Y. Zhao, J. Zhang, *J. Biosci. Bioeng.* **2010**, *110*, 53.
50. S. I. Miller, *mBio*. **2016**, *7*, e01541.
51. Z. V. Feng, I. L. Gunsolus, T. A. Qiu, K. R. Hurley, L. H. Nyberg, H. Frew, K. P. Johnson, A. M. Vartanian, L. M. Jacob, S. E. Lohse, M. D. Torelli, R. J. Hamers, C. J. Murphy, C. L. Haynes, *Chem. Sci.* **2015**, *6*, 5186.
52. D. M. Livermore, *J. Infect. Dis. Suppl.* **1990**, *74*, 15.
53. J. A. Kloepfer, R. E. Mielke, J. L. Nadeau, *Appl. Environ. Microbiol.* **2005**, *71*, 2548.
54. P. Demchick, A. L. Koch, *J. Bacteriol.* **1996**, *178*, 768.
55. T. G. Lonhienne, E. Sagulenko, R. I. Webb, K. C. Lee, J. Franke, D. P. Devos, A. Nouwens, B. J. Carroll, J. A. Fuerst, *Proc. Natl. Acad. Sci. U. S. A.* **2010**, *107*, 12883.
56. E. Navarro, A. Baun, R. Behra, N. B. Hartmann, J. Filser, A. J. Miao, A. Quigg, P. H. Santschi, L. Sigg, *Ecotoxicology* **2008**, *17*, 372.
57. D. K. Tripathi, A. Tripathi, Shweta, S. Singh, Y. Singh, K. Vishwakarma, G. Yadav, S. Sharma, V. K. Singh, R. K. Mishra, R. G. Upadhyay, N. K. Dubey, Y. Lee, D. K. Chauhan, *Front. Microbiol.* **2017**, *8*, 7.
58. J. R. Morones, J. L. Elechiguerra, A. Camacho, K. Holt, J. B. Kouri, J. T. Ramirez, M. J. Yacaman, *Nanotechnology* **2005**, *16*, 2346.
59. M. Kumar, W. Tegge, N. Wangoo, R. Jain, R. K. Sharma, *Biophys. Chem.* **2018**, *237*, 38.
60. S. Wang, R. Lawson, P. C. Ray, H. Yu, *Toxicol. Ind. Health* **2011**, *27*, 547.
61. Mohamed, M. M., S. A. Fouad, H. A. Elshoky, G. M. Mohammed, T. A. Salaheldin, *Int. J. Vet. Sci. Med.* **2017**, *5*, 23.
62. K. S. Butler, B. J. Casey, G. V. Garborcauskas, B. J. Dair, R. K. Elespuru, *Mutat. Res. Genet. Toxicol. Environ. Mutagen.* **2014**, *768*, 14.
63. W. Pajerski, D. Ochonska, M. Brzychczy-Wloch, P. Indyka, M. Jarosz, M. Golda-Cepa, Z. Sojka, A. Kotarba, *J. Nanopart. Res.* **2019**, *21*, 12.
64. E. Sawosz, A. Chwalibog, J. Szeliga, F. Sawosz, M. Grodzik, M. Rupiewicz, T. Niemiec, K. Kacprzyk, *Int. J. Nanomedicine* **2010**, *5*, 631.
65. H. Zhang, H. Liu, Z. Tian, D. Lu, Y. Yu, S. Cestellos-Blanco, K. K. Sakimoto, P. Yang, *Nat. Nanotechnol.* **2018**, *13*, 900.
66. S. Lara, F. Alnasser, E. Polo, D. Garry, M. C. Lo Giudice, D. R. Hristov, L. Rocks, A. Salvati, Y. Yan, K. A. Dawson, *ACS Nano* **2017**, *11*, 1884.
67. L. Boselli, E. Polo, V. Castagnola, K. A. Dawson, *Angew. Chem. Int. Ed.* **2017**, *56*, 4215.
68. J. C. Jin, X. J. Wu, J. Xu, B. B. Wang, F. L. Jiang, Y. Liu, *Biomater. Sci.* **2017**, *5*, 247.
69. M. Breisch, V. Grasmik, K. Loza, K. Pappert, A. Rostek, N. Ziegler, A. Ludwig, M. Heggen, M. Epple, J. C. Tiller, T. A. Schildhauer, M. Koller, C. Sengstock, *Nanotechnology* **2019**, *30*, 305101.
70. D. Pedone, M. Moglianetti, E. De Luca, G. Bardi, P. P. Pompa, *Chem. Soc. Rev.* **2017**, *46*, 4951.
71. L. Nejdl, J. Kudr, A. Moulick, D. Hegerova, B. Ruttkay-Nedecky, J. Gumulec, K. Cihalova, K. Smerkova, S. Dostalova, S. Krizkova, M. Novotna, P. Kopel, V. Adam, *PLoS One* **2017**, *12*, 19.
72. S. C. Hayden, G. Zhao, K. Saha, R. L. Phillips, X. Li, O. R. Miranda, V. M. Rotello, M. A. El-Sayed, I. Schmidt-Krey, U. H. F. Bunz, *J. Am. Chem. Soc.* **2012**, *134*, 6920.
73. S. K. Boda, J. Broda, F. Schiefer, J. Weber-Heynemann, M. Hoss, U. Simon, B. Basu, W. Jahnen-Dechent, *Small* **2015**, *11*, 3183.
74. A. Kotrbova, K. Stepka, M. Maska, J. J. Palenik, L. Ilkovics, D. Klemova, M. Kravec, F. Hubatka, Z. Dave, A. Hampl, V. Bryja, P. Matula, V. Pospichalova, *J. Extracell. Ves.* **2019**, *8*, 1560808.
75. X. Lai, M. L. Han, Y. Ding, S. H. Chow, A. P. Le Brun, C. M. Wu, P. J. Bergen, J. H. Jiang, H. Y. Hsu, B. W. Muir, J. White, J. Song, J. Li, H. H. Shen, *Nat. Commun.* **2022**, *13*, 343.
76. P. V. Baptista, M. P. McCusker, A. Carvalho, D. A. Ferreira, N. M. Mohan, M. Martins, A. R. Fernandes, *Front. Microbiol.* **2018**, *9*, 1441.
77. L. Zhang, D. Pornpattananangkul, C. M. Hu, C. M. Huang, *Curr. Med. Chem.* **2010**, *17*, 585.
78. A. Ranjan, N. Pothayee, M. N. Seleem, R. D. J. Tyler, B. Brenseke, N. Sriranganathan, J. S. Riffle, R. Kasimanickam, *Int. J. Nanomedicine* **2009**, *4*, 289.
79. G. Mohammadi, H. Valizadeh, M. Barzegar-Jalali, F. Lotfipour, K. Adibkia, M. Milani, M. Azhdarzadeh, F. Kiafar, A. Nokhodchi, *Colloids Surf. B Biointerfaces* **2010**, *80*, 34.
80. G. Mohammadi, A. Nokhodchi, M. Barzegar-Jalali, F. Lotfipour, K. Adibkia, N. Ehyaei, H. Valizadeh, *Colloids Surf. B Biointerfaces* **2011**, *88*, 39.
81. V. Castro, H. Rodriguez, F. Albericio, *ACS Combinat. Sci.* **2016**, *18*, 1.
82. J. E. Hein, V. V. Fokin, *Chem. Soc. Rev.* **2010**, *39*, 1302.
83. F. Angius, O. Ilioaia, A. Amrani, A. Suisse, L. Rosset, A. Legrand, A. Abou-Hamdan, M. Uzan, F. Zito, B. Miroux, *Sci. Rep.* **2018**, *8*, 8572.
84. S. Stumpf, G. Hostnik, M. Primozic, M. Leitgeb, U. Bren, *Plants* **2020**, *9*, 1680.

85. M. Rosenberg, N. F. Azevedo, A. Ivask, *Sci. Rep.* **2019**, *9*, 6483.
86. M. J. Rust, M. Bates, X. Zhuang, *Nat. Meth.* **2006**, *3*, 793.
87. L. Turner, W. S. Ryu, H. C. Berg, *J. Bacteriol.* **2000**, *182*, 2793.
88. R. Wirth, A. Bellack, M. Bertl, Y. Bilek, T. Heimerl, B. Herzog, M. Leisner, A. Probst, R. Rachel, C. Sarbu, S. Schopf, G. Wanner, *Appl. Environ. Microbiol.* **2011**, *77*, 1556.
89. L. Rojas-Sanchez, K. Loza, M. Epple, *Materialia* **2020**, *12*, 100773.

How to cite this article: N. Białas, V. Sokolova, S. B. van der Meer, T. Knuschke, T. Ruks, K. Klein, A. M. Westendorf, M. Epple, *Nano Select*. **2022**, *3,* 1407. https://doi.org/10.1002/nano.202200049

DOI: 10.1002/nano.202200049
URN: urn:nbn:de:hbz:465-20231120-143525-1